Correction of Arbitrary Field Errors in Population Inversion of Quantum Systems by Universal Composite Pulses

Genko T. Genov,[1,2] Daniel Schraft,[2] Thomas Halfmann,[2] and Nikolay V. Vitanov[1]
[1]Department of Physics, St. Kliment Ohridski University of Sofia, 5 James Bourchier boulevard, 1164 Sofia, Bulgaria
[2]Institut für Angewandte Physik, Technische Universität Darmstadt, Hochschulstraße 6, 64289 Darmstadt, Germany
(Received 19 March 2014; revised manuscript received 22 May 2014; published 22 July 2014)

We introduce universal broadband composite pulse sequences for robust high-fidelity population inversion in two-state quantum systems, which compensate deviations in any parameter of the driving field (e.g., pulse amplitude, pulse duration, detuning from resonance, Stark shifts, unwanted frequency chirp, etc.) and are applicable with any pulse shape. We demonstrate the efficiency and universality of these composite pulses by experimental data on rephasing of atomic coherences in a Pr^{3+}:Y_2SiO_5 crystal.

DOI: 10.1103/PhysRevLett.113.043001 PACS numbers: 32.80.Qk, 32.80.Xx, 42.50.Md, 82.56.Jn

Performing high-fidelity and robust population transfer by external fields remains an important challenge in various areas of physics, e.g., atomic and molecular physics [1], nuclear magnetic resonance [2], and quantum information processing [3–5]. Most of the available techniques provide either high population transfer efficiency or robustness against variations in the field parameters, but not both. For example, resonant techniques deliver high efficiency but are not robust. Adiabatic passage techniques [6–8] are robust, but in nearly all of them population transfer is incomplete and very long interaction times and/or high intensities are required to satisfy the adiabaticity criteria. Optimal control techniques [1,9], including the emerging field of "shortcuts to adiabaticity" [10], achieve high fidelity by tailoring the time dependences of the amplitude and the phase of the driving field. However, their implementation is often challenging because they usually prescribe rather demanding time dependences, while various experimental limitations (field inhomogeneities, spatial pulse shape distortion, etc.) can limit their efficiency.

The technique of composite pulses (CPs) is far easier to implement and has been used for decades in nuclear magnetic resonance [2] and, since recently, in quantum information processing [3–5,11] and quantum optics [12–16] for highly accurate and robust qubit rotation. CPs are unique in combining the advantages of resonant techniques (very high fidelity) and adiabatic techniques (robustness to errors). The basic idea of CPs is to correct the imperfect interaction of a quantum system with a single pulse by using a sequence of pulses with suitably chosen relative phases, which are usually easy to control experimentally. The errors introduced by the constituent pulses are canceled by destructive interference up to a certain order.

In this Letter, we describe a general theoretical procedure to derive universal CPs for complete population inversion, which compensate deviations in any experimental parameter and work with any pulse shape. Essentially, all of the existing CPs compensate errors in a single interaction parameter, or at most two interaction parameters, and usually assume a rectangular pulse shape. The only assumptions made here are those of a two-state system, coherent evolution, and identical pulses in the CP sequence [17]. As a basic example of relevance to many applications in quantum physics, we experimentally demonstrate the concept by rephasing of atomic coherences for optical data storage in a Pr^{3+}:Y_2SiO_5 crystal.

We consider a coherently driven two-state quantum system. Its dynamics obeys the Schrödinger equation, $i\hbar\partial_t\mathbf{c}(t)=\mathbf{H}(t)\mathbf{c}(t)$, where the vector $\mathbf{c}(t)=[c_1(t),c_2(t)]^T$ contains the probability amplitudes of the two states. The Hamiltonian in the rotating-wave approximation reads $\mathbf{H}(t)=(\hbar/2)\Omega(t)e^{-i\delta(t)}|1\rangle\langle 2|+\text{H.c.}$, with $\delta(t)=\int_0^t\Delta(t')dt'$, where $\Delta=\omega_0-\omega$ is the detuning between the field frequency ω and the Bohr transition frequency ω_0. The Rabi frequency $\Omega(t)=-\mathbf{d}\cdot\mathbf{E}(t)/\hbar$ defines the coupling of the two states, induced by the electric field $\mathbf{E}(t)$ and the transition dipole moment $\mathbf{d}$. In general, both $\Omega(t)$ and $\Delta(t)$ are time dependent.

We assume that the CP duration is shorter than the decoherence times in the system. Then, the evolution is described by the propagator $\mathbf{U}$, which connects the amplitudes at the initial and final times t_i and t_f: $\mathbf{c}(t_f)=\mathbf{U}\mathbf{c}(t_i)$. It is conveniently parametrized with the three real Stückelberg variables q $(0\leqq q\leqq 1)$, α, and β as

$$\mathbf{U}=\begin{bmatrix} qe^{i\alpha} & pe^{i\beta} \\ -pe^{-i\beta} & qe^{-i\alpha}\end{bmatrix}, \tag{1}$$

where $p=\sqrt{1-q^2}$; p^2 is the transition probability from state $|1\rangle$ to state $|2\rangle$, and q^2 is the probability for no transition. A constant phase shift ϕ in the Rabi frequency, $\Omega(t)\to\Omega(t)e^{i\phi}$, is imprinted in the propagator $\mathbf{U}(\phi)$ by taking $\beta\to\beta+\phi$ [13]. The propagator for a composite sequence of n pulses, each with a phase ϕ_k, reads

$$\mathbf{U}^{(n)}=\mathbf{U}(\phi_n)\cdots\mathbf{U}(\phi_2)\mathbf{U}(\phi_1), \tag{2}$$

where the phases $\phi_1,\dots,\phi_n$ are free control parameters.

Our objective is to transfer all population from state $|1\rangle$ to state $|2\rangle$, even when the properties of the driving pulse are *unknown*. This requires robustness to deviations in all pulse parameters, i.e., pulse shape, Rabi frequency, duration, detuning from resonance, dynamic Stark shifts, residual frequency chirp, etc. Mathematically, our goal is to maximize the transition probability $P^{(n)} = |U_{21}^{(n)}|^2$, i.e., to minimize the CP infidelity (the probability for no transition) $Q^{(n)} = |U_{11}^{(n)}|^2$ for any values of q, α, and β. We make no assumptions about the constituent pulses, i.e., how q, α, and β depend on the interaction parameters. This justifies the term "universal" for these CPs because they will compensate imperfections in any interaction parameter. We assume only that the constituent pulses are identical and that we have control over their phases ϕ_k.

In order to determine the phases ϕ_k of a universal CP sequence of n pulses we calculate the propagator element $U_{11}^{(n)}$ from Eq. (2). We find $U_{11}^{(n)} = \sum_{j=1}^{n} c_{nj} q^j$, where the coefficients c_{nj} depend on α and ϕ_k only. Following arguments in Refs. [13,14] we use symmetric CPs, the phases of which obey the anagram relation $\phi_{n+1-k} = \phi_k$, with $k = 1, 2, \ldots, (n-1)/2$. Such symmetric sequences automatically nullify all c_{nj} for even j. We choose phases such that the coefficients c_{nj} are nullified for any α up to the highest possible order, denoted j_0. This generates a system of trigonometric equations for the phases ϕ_k. In general, there are multiple solutions. We choose solutions, which minimize the sum of the absolute values of the coefficients of the first nonzero order $j_0 + 1$. The transition probability for such CP reads $P^{(n)} = 1 - |U_{11}^{(n)}|^2 = 1 - O(q^{2j_0+2})$. Since $0 \leqq q \leqq 1$, we can make the error term arbitrary small (unless $q = 1$, which means zero transition probability for a single pulse) by nullifying c_{nj} to an arbitrary high order j_0 by using longer composite sequences. For example, for a five-pulse sequence, we have $U_{11}^{(5)} = \{[1 + 2\cos(2\phi_2 - \phi_3)]e^{i\alpha} + 2\cos(\phi_2 - \phi_3)e^{-i\alpha}\}q + O(q^3)$. The q term vanishes for two distinct sets: $\{\phi_2 = 5\pi/6, \phi_3 = \pi/3\}$ and $\{\phi_2 = 11\pi/6, \phi_3 = \pi/3\}$. Then, we have $j_0 = 2$ and $P^{(n)} = 1 - |U_{11}^{(5)}|^2 = 1 - O(q^6)$.

Several universal CPs are listed in Table I. The CPs labeled "*a*" perform better against variations in the pulse area (i.e., pulse duration and amplitude), whereas those labeled "*b*" perform better against the static detuning. Either of these, however, permit compensation against both parameters, as well as against any other parameters. The CPs $U5a$ and $U5b$ in Table I were derived earlier, aiming at compensation of pulse area [18] and detuning errors [13] for specific pulse shapes. To the best of our knowledge, all other universal CPs in Table I were not known before.

Figure 1 depicts the theoretical performance of a single pulse and universal CPs up to order 25 of types "*a*" and "*b*" against the static detuning and the duration T of each constituent pulse. As it is well known, the transition probability for a single pulse quickly drops when T does not match to a perfect π pulse, i.e., $T = \tau$, or when the pulse carrier frequency is off resonance. We plotted the error $|U_{11}^{(n)}|^2$ and we used a logarithmic scale to verify the suitability of these CPs for applications requiring ultrahigh fidelity, e.g., as in quantum information processing. The universal CP sequences are robust with respect to variations along both axes. Furthermore, the 10^{-4} error regions are far broader than for a single pulse, and they expand steadily with the CP order.

TABLE I. Phases of universal CPs with n pulses (indicated by the number in the label of the CP). We have $j_0 = 0$ for $n = 3$, $j_0 = 2$ for $n = 5$ to 9, $j_0 = 4$ for $n = 13$, and $j_0 = 8$ for $n = 25$. Each phase is defined modulo 2π. The excitation dynamics remain the same when we simultaneously change the sign of all phases or add a constant shift to all phases.

Pulse	Phases
$U3$	$(0, 1, 0)\pi/2$
$U5a$	$(0, 5, 2, 5, 0)\pi/6$
$U5b$	$(0, 11, 2, 11, 0)\pi/6$
$U7a$	$(0, 11, 10, 17, 10, 11, 0)\pi/12$
$U7b$	$(0, 23, 10, 5, 10, 23, 0)\pi/12$
$U9a$	$(0, 0.635, 1.35, 0.553, 0.297, 0.553, 1.35, 0.635, 0)\pi$
$U9b$	$(0, 1.635, 1.35, 1.553, 0.297, 1.553, 1.35, 1.635, 0)\pi$
$U13a$	$(0, 9, 42, 11, 8, 37, 2, 37, 8, 11, 42, 9, 0)\pi/24$
$U13b$	$(0, 33, 42, 35, 8, 13, 2, 13, 8, 35, 42, 33, 0)\pi/24$
$U25a$	$(0, 5, 2, 5, 0, 11, 4, 1, 4, 11, 2, 7, 4, 7, 2, 11, 4, 1, 4, 11, 0, 5, 2, 5, 0)\pi/6$
$U25b$	$(0, 11, 2, 11, 0, 5, 4, 7, 4, 5, 2, 1, 4, 1, 2, 5, 4, 7, 4, 5, 0, 11, 2, 11, 0)\pi/6$

We experimentally verified the performance of the universal CP sequences by rephasing atomic coherences for optical data storage. In the experiment, we generate the atomic coherence on a magnetic, radio-frequency (rf) transition between two inhomogeneously broadened hyperfine levels of $Pr^{3+}{:}Y_2SiO_5$ crystal. The atomic coherence between the two quantum states is prepared and read out by electromagnetically induced transparency (EIT) [19]. This enables straightforward, on-demand optical readout. The EIT scheme couples states $|1\rangle$ and $|2\rangle$ by a strong control field and a weak probe field via an excited state $|3\rangle$. By simultaneously and adiabatically turning off the control and probe fields, we convert the probe field into an atomic coherence, i.e., a coherent superposition of states $|1\rangle$ and $|2\rangle$. This is the "write" process of optical information encoded in the probe field, often termed "stopped light" or "stored light" [19]. To "read" the optical memory after an arbitrary storage time, we apply the strong control field again to beat with the atomic coherence and thereby generate a signal field with the same properties as the stored field. The concept and the experimental setup for EIT-based light storage in $Pr^{3+}{:}Y_2SiO_5$ are described in detail elsewhere [8,15,20].

In such a coherent optical memory it is crucial to reverse the effect of dephasing of the atomic coherences during the storage time. The dephasing is due to inhomogeneous broadening of the hyperfine levels, while rephasing is implemented usually by resonant rf π pulses. However,

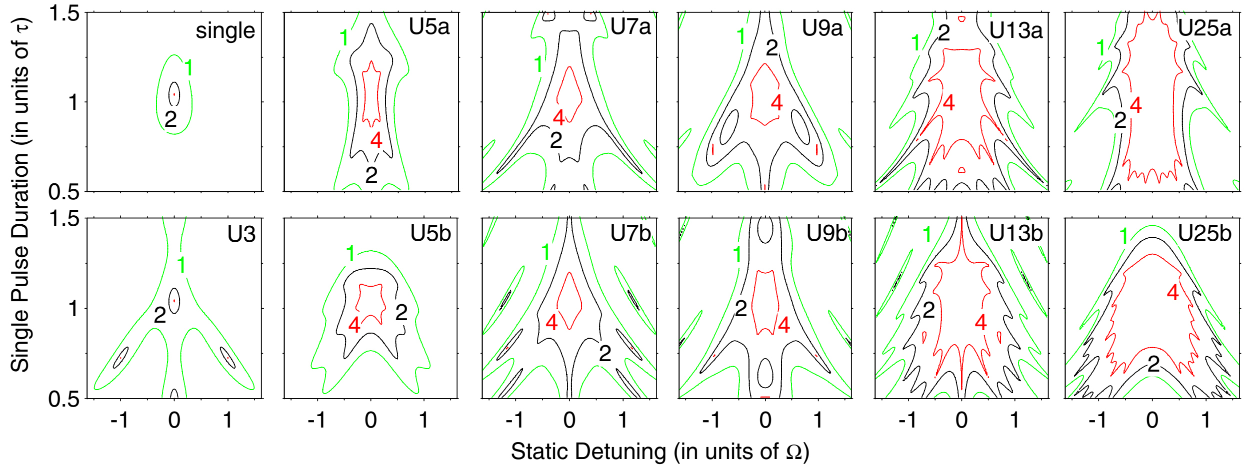

FIG. 1 (color online). Numerically simulated infidelity $|U_{11}^{(n)}|^2$ vs static detuning and duration T of each constituent pulse (referred to as "single pulse duration") for a single pulse and several universal CPs (with rectangular shapes) from Table I. The labels $m = 1, 2, 4$ indicate the error level 10^{-m}.

such pulses do not work efficiently in systems with large inhomogeneous broadening, as the transition frequency varies for different ions. The efficiency is further reduced by the spatial inhomogeneity of the rf field over the crystals dimensions. In order to permit a much broader operation bandwidth, we replace now the single π pulses by our universal CPs, similarly to Ref. [15]. In the experiment we set the storage time to 600 μs, which is much larger than the dephasing time of about 20 μs. During this storage time we rephase the atomic coherence by applying a pair of (composite) pulses, where the first (composite) pulse is centered at 150 μs and the second at 450 μs. The optical "write" and "read" sequences were kept fixed, while the rf rephasing sequences were varied; therefore, the energy of the retrieved signal measures the rephasing efficiency, and hence, the efficiency of the driving single pulses or universal CPs.

Figure 2 compares the theoretical performance and experimental results for a single pulse and the universal CP $U3$ versus variations in the single pulse duration and static detuning. We note that in Figs. 2(a) and 2(b), in contrast to Fig. 1, we have simulated $|U_{21}^{(n)}|^4$, i.e., the rephasing efficiency, averaged over all possible stored coherences. The experimental data [Figs. 2(c) and 2(d)] agree remarkably well with the numerical simulations, and fully confirm the pronounced robustness of the universal CP sequences.

Next, we experimentally compare the behavior of universal CP sequences of orders $n = 3$, 5, 7, 9 in Fig. 3. We apply CPs with rectangular (R) and Gaussian (G) temporal shape (left and right columns in Fig. 3). The data for the universal CP sequence $U3$ R, already shown in Fig. 2(d), serve as a benchmark. As the data clearly show, the robustness of all universal CP sequences to variations in the experimental parameters is much larger compared to a single pulse [Fig. 2(c)]. As expected, the region of large rephasing efficiency increases with the order of the universal CP sequences. The behavior is the same for rectangular and Gaussian pulses; i.e., the optimal phases in the CP sequence do not depend on the pulse shape. The experimental data clearly confirm the theoretical predictions: indeed, the overall shapes of the high-efficiency regions in Fig. 3 look remarkably similar to the theoretical plots in Fig. 1. The "duck-foot" pattern for $U3$, the "boomerang" pattern for $U5b$, and the "pine-tree" pattern for $U7b$ are very nicely reproduced.

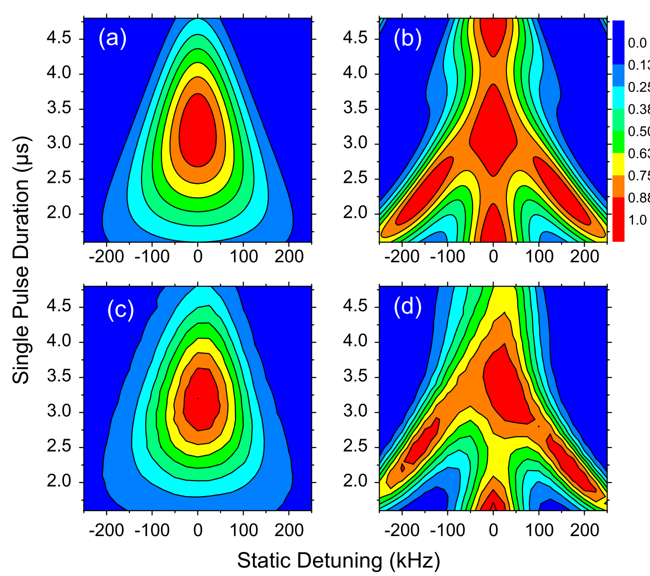

FIG. 2 (color online). Numerically simulated (a),(b) and experimentally measured rephasing efficiency of stored light (c),(d) vs static detuning and single pulse duration T for a single rectangular pulse (a),(c) and rectangular CP $U3$ (b),(d) with phases (0, $\pi/2$, 0) from Table I. The Rabi frequency is kept fixed at $\Omega_{rf} \approx 2\pi \times 155$ kHz; i.e., a single π pulse has a duration of $\tau = 3.2$ μs.

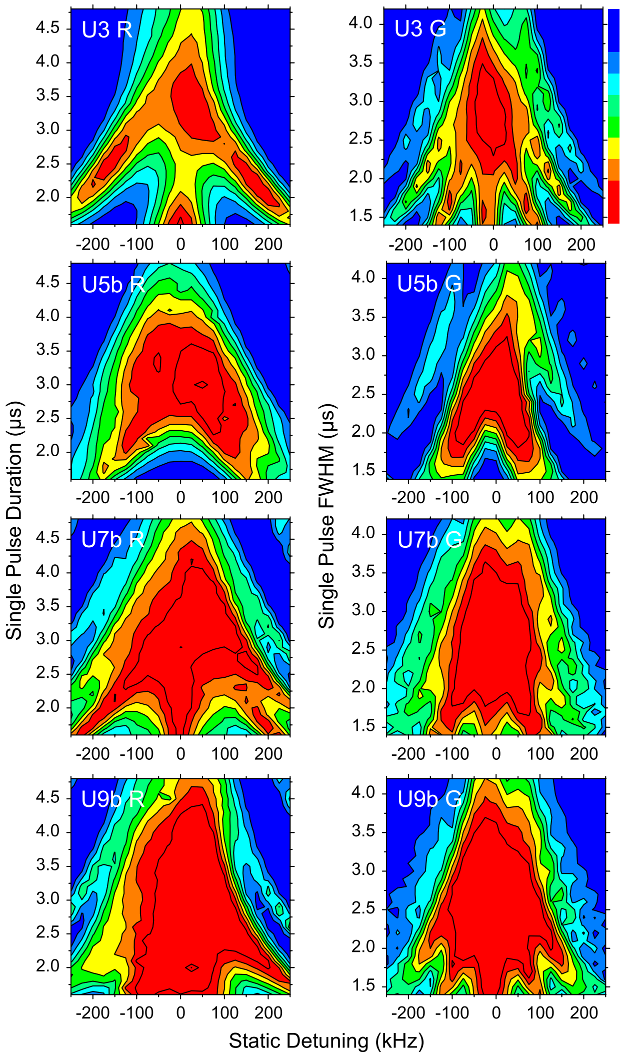

FIG. 3 (color online). Experimentally measured rephasing efficiency of stored light vs static detuning and single pulse duration for different universal CP sequences from Table I (labeled in each frame). The left column is for sequences of rectangular pulses and the right column is for sequences of Gaussian pulses. In either case the peak Rabi frequency is $\Omega_{rf} \approx 2\pi \times 155$ kHz. Hence, for rectangular pulses, the pulse duration of a perfect π pulse is $\tau = 3.2\ \mu$s and for Gaussian pulses, it is 2.8 μs (FWHM).

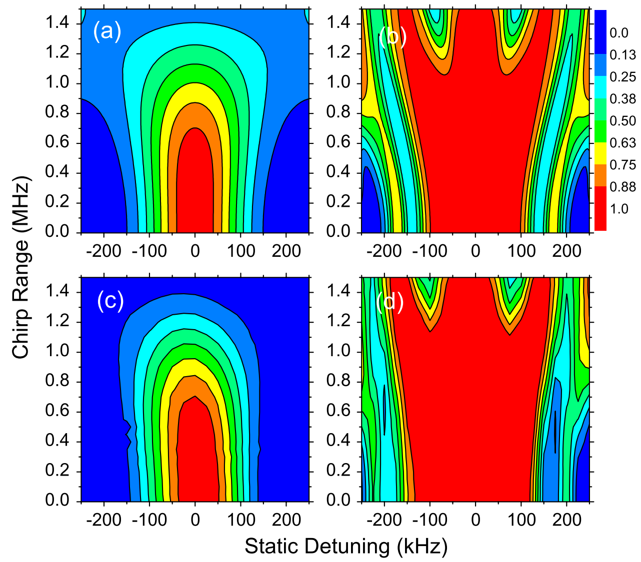

FIG. 4 (color online). Numerically simulated (a),(b) and experimentally measured rephasing efficiency of stored light (c),(d) vs static detuning and chirp range, symmetric around resonance, of each constituent pulse for a single rectangular pulse (a),(c) and universal CP $U9b$ with phases from Table I (b),(d). The Rabi frequency is kept fixed at $\Omega_{rf} \approx 2\pi \times 155$ kHz and the duration of each (constituent) pulse is $T = 3.2\ \mu$s.

We also verified by extensive simulations the robustness of the universal CPs against variations in other interaction parameters, e.g., Stark shifts, unwanted frequency chirp, pulse shape, etc. All simulations confirm that our universal CPs are amazingly robust to any such variation. For example, Fig. 4 shows a comparison of the rephasing efficiency of a pair of single pulses and a pair of $U9b$ CPs, given in Table I, versus the frequency chirp range and the static detuning. In this example, we applied a linear chirp, symmetric around resonance, on each constituent pulse. Figures 4(a) and 4(c) show that the efficiency of a single pulse quickly drops with static detunings larger than 50 kHz and chirp ranges larger than 700 kHz. In comparison, the CP $U9b$ sequence in Figs. 4(b) and 4(d) features a much better stability against variations in both axes. The experimental data agree remarkably well with the numerical simulations and fully confirm the pronounced robustness of the universal CP sequences.

In conclusion, we theoretically developed and experimentally demonstrated universal broadband CP sequences for robust high-fidelity population inversion. These CPs compensate simultaneous variations in *all* experimental parameters (e.g., intensity or Rabi frequency, pulse duration, static detuning, Stark shifts, frequency chirp, etc.) and are applicable with any pulse shape. We experimentally confirmed the theoretical predictions by rephasing atomic coherences in a Pr^{3+}:Y_2SiO_5 crystal. In particular, our data demonstrate robust rephasing in a broad range of experimental parameters and for different pulse shapes. The efficiency and operation bandwidth of universal CPs are significantly larger compared to conventional π pulses or nonuniversal CPs. The universal CPs will be a highly accurate and robust tool for quantum control, particularly valuable in the presence of significant experimental uncertainties.

This work is supported by the Deutsche Forschungsgemeinschaft, the Alexander von Humboldt Foundation, and the European Union's Seventh Framework Programme under REA Grant No. 287252.

G. T. G. and D. S. contributed equally to the results presented in this Letter.

[1] C. Brif, R. Chakrabarti, and H. Rabitz, New J. Phys. **12**, 075008 (2010); S. Rice and M. Zhao, *Optimal Control of Quantum Dynamics* (Wiley, New York, 2000); M. Shapiro and P. Brumer, *Principles of Quantum Control of Molecular Processes* (Wiley, New York, 2003); D. J. Tannor, *Introduction to Quantum Mechanics: A Time-Dependent Perspective* (University Science Books, Sausalito, CA, 2007).

[2] M. H. Levitt, Prog. Nucl. Magn. Reson. Spectrosc. **18**, 61 (1986); R. Freeman, *Spin Choreography* (Spektrum, Oxford, 1997).

[3] F. Schmidt-Kaler, H. Häffner, M. Riebe, S. Gulde, G. P. T. Lancaster, T. Deuschle, C. Becher, C. F. Roos, J. Eschner and R. Blatt, Nature (London) **422**, 408 (2003); M. Riebe, T. Monz, A. S. Villar, P. Schindler, M. Chwalla, M. Hennrich, and R. Blatt, Nat. Phys. **4**, 839 (2008); T. Monz, K. Kim, W. Hänsel, M. Riebe, A. S. Villar, P. Schindler, M. Chwalla, M. Hennrich, and R. Blatt, Phys. Rev. Lett. **102**, 040501 (2009).

[4] M. Pons, V. Ahufinger, C. Wunderlich, A. Sanpera, S. Braungardt, A. Sen(De), U. Sen, and M. Lewenstein, Phys. Rev. Lett. **98**, 023003 (2007); N. Timoney, V. Elman, S. Glaser, C. Weiss, M. Johanning, W. Neuhauser, and C. Wunderlich, Phys. Rev. A **77**, 052334 (2008); C. Piltz, B. Scharfenberger, A. Khromova, A. F. Varon, and C. Wunderlich, Phys. Rev. Lett. **110**, 200501 (2013).

[5] C. D. Hill, Phys. Rev. Lett. **98**, 180501 (2007).

[6] N. V. Vitanov, T. Halfmann, B. W. Shore and K. Bergmann, Annu. Rev. Phys. Chem. **52**, 763 (2001).

[7] M. F. Pascual-Winter, R. C. Tongning, R. Lauro, A. Louchet-Chauvet, T. Chanelière, and J.-L. Le Gouët, Phys. Rev. B **86**, 064301 (2012).

[8] S. Mieth, D. Schraft, T. Halfmann, and L. P. Yatsenko, Phys. Rev. A **86**, 063404 (2012).

[9] L. S. Pontryagin, V. G. Boltyanskii, R. V. Gamkrelidze, and E. F. Mishchenko, *The Mathematical Theory of Optimal Processes* (Mir, Moscow, 1974); B. Bonnard and M. Chyba, *Singular Trajectories and Their Role in Control Theory* (Springer, New York, 2003), Vol. 40.

[10] M. Demirplak and S. A. Rice, J. Phys. Chem. A **107**, 9937 (2003); M. V. Berry, J. Phys. A **42**, 365303 (2009).

[11] S. S. Ivanov and N. V. Vitanov, Phys. Rev. A **84**, 022319 (2011).

[12] S. S. Ivanov and N. V. Vitanov, Opt. Lett. **36**, 1275 (2011); G. T. Genov, B. T. Torosov, and N. V. Vitanov, Phys. Rev. A **84**, 063413 (2011); G. T. Genov and N. V. Vitanov, Phys. Rev. Lett. **110**, 133002 (2013).

[13] B. T. Torosov and N. V. Vitanov, Phys. Rev. A **83**, 053420 (2011).

[14] B. T. Torosov, S. Guérin, and N. V. Vitanov, Phys. Rev. Lett. **106**, 233001 (2011).

[15] D. Schraft, T. Halfmann, G. T. Genov, and N. V. Vitanov, Phys. Rev. A **88**, 063406 (2013).

[16] B. T. Torosov and N. V. Vitanov, Phys. Rev. A **87**, 043418 (2013).

[17] We point out that this method compensates only errors in the driving field and should not be confused with quantum error correction, which protects from errors due to decoherence and other quantum noise stemming from the environment.

[18] R. Tycko and A. Pines, Chem. Phys. Lett. **111**, 462 (1984).

[19] M. Fleischhauer, A. Imamoglu, and J. P. Marangos, Rev. Mod. Phys. **77**, 633 (2005).

[20] G. Heinze, C. Hubrich, and T. Halfmann, Phys. Rev. Lett. **111**, 033601 (2013).